Colloids and Surfaces A: Physicochemical and Engineering Aspects 702 (2024) 135105

Contents lists available at ScienceDirect

Colloids and Surfaces A: Physicochemical and Engineering Aspects

journal homepage: www.elsevier.com/locate/colsurfa

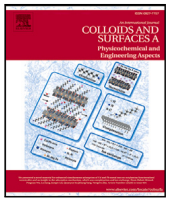

PNIPAM microgel coatings of LiF crystal radiation detectors

Valentina Nigro [a,b,*], Claudia Colantonio [b], Massimo Piccinini [a], Elena Buratti [c,b], Riccardo Ciciotti [d], Evaristo Cisbani [e], Cinzia De Angelis [e], Franco Dinelli [f], Giuseppe Esposito [e], Francesca Limosani [g], Enrico Nichelatti [g], Concetta Ronsivalle [a], Maria Aurora Vincenti [a], Barbara Ruzicka [b,h], Rosa Maria Montereali [a]

[a] ENEA C.R. Frascati, Nuclear Department, Via Enrico Fermi 45, Frascati (Rome), 00044, Italy
[b] Institute for Complex Systems, National Research Council (ISC-CNR), sede Sapienza University, P.le Aldo Moro 2, Rome, 00185, Italy
[c] Department of Chemical, Pharmaceutical and Agricultural Sciences, University of Ferrara, Via Luigi Borsari, 46, Ferrara, 14412, Italy
[d] Department of Physics, University of Rome "Tor Vergata", Via della ricerca scientifica, 1, Rome, 00133, Italy
[e] Istituto Superiore di Sanità, Viale Regina Elena 299, Rome, 00161, Italy
[f] National Institute of Optics (INO-CNR), via Moruzzi 1, Pisa, 56124, Italy
[g] ENEA C.R. Casaccia, Nuclear Department, Via Anguillarese, 301, Santa Maria di Galeria (Rome), 00123, Italy
[h] Department of Physics, Sapienza University, P.le Aldo Moro 2, Rome, 00185, Italy

GRAPHICAL ABSTRACT

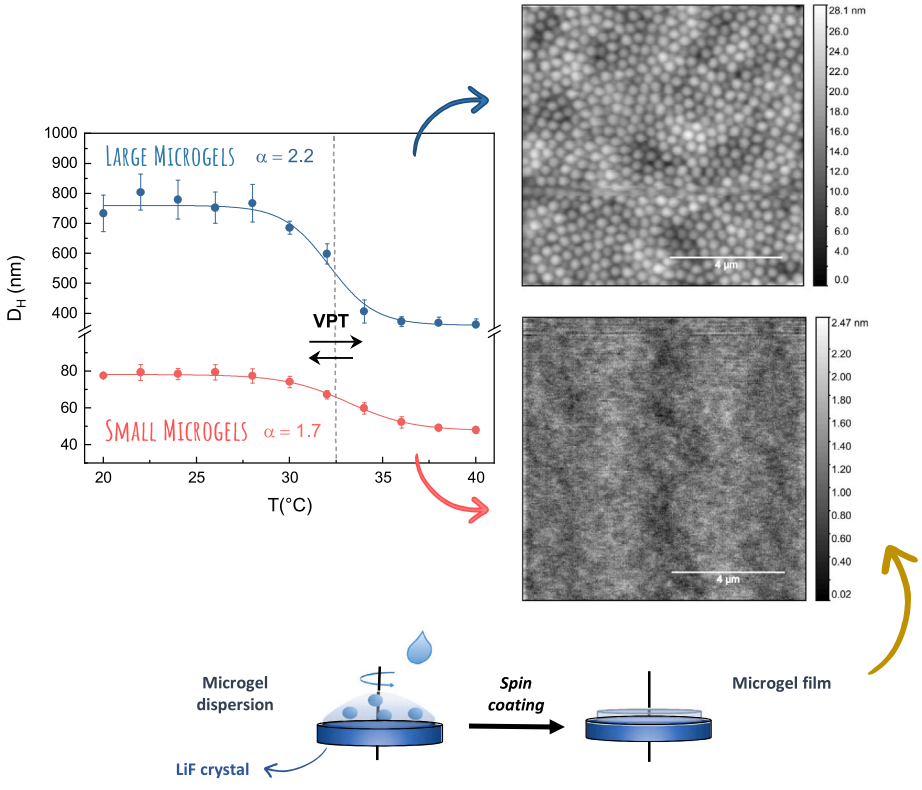

* Corresponding author at: ENEA C.R. Frascati, Nuclear Department, Via Enrico Fermi 45, Frascati (Rome), 00044, Italy.
E-mail address: valentina.nigro@enea.it (V. Nigro).

https://doi.org/10.1016/j.colsurfa.2024.135105
Received 16 April 2024; Received in revised form 9 August 2024; Accepted 12 August 2024
Available online 14 August 2024

ARTICLE INFO

Keywords:
Thin films
Microgels
PNIPAM
Fluorescent nuclear track detectors

ABSTRACT

Thin films of poly(N-isopropylacrylamide) (PNIPAM) microgels have recently attracted significant attention as promising candidates for creating switchable interfaces in biomedical and biotechnological applications. In this study, microgel films are proposed as smart coatings for photoluminescent solid-state radiation detectors based on lithium fluoride (LiF). Understanding the impact of the solid substrate is crucial for customising and refining microgel coatings for specific applications. To investigate the effects of surface quality, microgel size, and particle concentration on the properties of microgel films, PNIPAM microgels were spin-coated onto LiF crystal surfaces and characterised through wettability measurements, UV-Vis-NIR spectrophotometry, and Atomic Force Microscopy. This approach enabled effective control over the optical and morphological properties of the films, paving the way for the development of hybrid and potentially biocompatible radiation detectors using PNIPAM microgel films.

1. Introduction

Thin films of polymeric microgels have attracted significant interest in recent years due to their unique properties and versatile applications. Microgels, typically composed of cross-linked polymer networks, are colloidal particles that can swell or shrink in response to external stimuli such as temperature, pH, or ionic strength [1–3]. When organised into films, these microgels exhibit unique properties with applications across different fields thanks to their fascinating optical and morphological properties [4,5].

In particular, polymeric microgels based on poly(N-isopropylacrylamide) (PNIPAM), are especially attractive for biomedical and biotechnological applications. PNIPAM microgels are indeed thermoresponsive particles showing a reversible Volume Phase Transition (VPT) in response to temperature changes, specifically around the lower critical solution temperature of the polymer, approximately of 32 °C. As a result of this temperature-responsiveness, PNIPAM-based microgels exhibit a transition from a swollen to a collapsed state across the VPT Temperature (VPTT) that can be harnessed to fabricate smart materials with controlled drug release, sensing, and responsive surface properties [6,7].

Thin films of PNIPAM microgels have been recently investigated as promising candidates for fabricating switchable interfaces for different technological applications, including sensing [8–10], bio-sensing [11,12] and tissue engineering [4,13]. In particular, PNIPAM microgel films have been proposed as smart substrates to control cell growth and detachment via temperature stimuli to minimise the impact of enzymatic and chemical treatments usually used for cell detachment [14,15]. Moreover, microgel films can be exploited to couple technological devices with biological systems. Indeed, their ability to easily tune and adapt on interfaces makes microgels fascinating building blocks for fabricating smart and biocompatible surfaces [16,17].

In this work we present an innovative application of microgel-based films as smart coatings of photoluminescent solid-state radiation detectors widely used for advanced diagnostics of proton beams. Indeed in the last years many efforts have been spent for simultaneous assessment of biological response and beam energy deposition parameters with a high spatial resolution. The quantitative measurement of ion spatial distribution and the average dose locally delivered to single cells is imperative to evaluate the damage induced by ionising radiations on biological tissues and living organisms. In this framework, Fluorescent Nuclear Track Detectors (FNTDs) attracted great interest since they provide local information on energy deposition from single protons and heavy ions.

Recently, FNTDs based on lithium fluoride (LiF) have been proposed as novel passive integrating radiation detectors [18–20]. Lithium fluoride is an alkali halide well known as active laser medium and as thermoluminescent dosimeter that is sensitive to different ionising radiations, such as electrons, X-rays, gamma rays, protons and heavy ions, inducing the stable formation of photoluminescent electronic defects in the material, known as colour centres (CCs) [21,22]. When excited with blue light, some of these aggregate centres emit a broad spectrum of visible light consisting of two bands peaked around 670 nm (F_2 centres) and 525 nm (F_3^+ centres), whose intensities are proportional to the energy deposited in the material by the ionising radiation. Their photoluminescence is well known for applications in optically-pumped tunable lasers [23], broad-band miniaturised light-emitting photonic devices [24], and passive X-ray imaging detectors [25] with high spatial resolution. In the last decade, exploitation of the photoluminescence of these radiation-induced aggregate defects has been proposed for proton beam advanced diagnostics and dosimetry [26,27], even at dose values typical of radiotherapy [28]. Exploiting their high spatial resolution, LiF-based FNTDs allow for the imaging of single charged particle paths within the material and the exact measurement of the number of incident ions, their direction and the energy deposited by each single proton [18]. Coating the FNTD surface with cell layers recently emerged as a successful strategy aiming at extrapolating single fluorescent tracks of protons and ions into the attached cell layer with subcellular accuracy [29,30].

Smart coatings based on PNIPAM microgels have been therefore proposed to develop hybrid detectors able to combine the high spatial resolution of LiF-based FNTDs with the PNIPAM biocompatibility to efficiently couple cell layers with the radiation detector surface. These detectors aim to directly correlate the information of locally-delivered radiation dose and the cell response in order to investigate the molecular mechanism of radiobiological response to particle therapy. In this framework, the influence of the solid substrate on the microgel coatings is a crucial aspect that significantly affects both the properties and performances of the resulting coated material. Optimising factors such as wettability and surface energy, roughness, and chemical composition can enhance microgel adhesion, thus ensuring a stable and durable coating [31–34].

In the present manuscript we report a systematic investigation of PNIPAM microgel films deposited on LiF crystals by combining wettability measurements, UV-Vis-NIR spectrophotometry and Atomic Force Microscopy in order to understand the influence of the solid substrate for tailoring microgel coatings to specific applications. Indeed, the knowledge of the substrate will help to optimise the coating and to unlock new possibilities for microgel-coated materials, especially when used for biomedical devices, sensors, or responsive surfaces.

2. Experimental methods

2.1. Materials

N-isopropylacrylamide (NIPAM), N,N'-methylene-bis-acrylamide (BIS), potassium persulfate (KPS) (98% purity) were purchased from Sigma-Aldrich. NIPAM monomer and BIS, used as cross-linker, were recrystallised from hexane and methanol respectively, dried under reduced pressure (0.01 mmHg) at room temperature and stored at 20 °C. KPS, employed as initiator, and sodium dodecyl sulfate (SDS),

Table 1
Spin speeds of the first and second steps of the deposition protocols for thin films of PNIPAM microgels spin-coated on LiF crystals.

Protocol	ω_1 (rpm)	ω_2 (rpm)
1	1500	5000
2	500	5000

employed as surfactant, were used as received. Also all the other solvents (Sigma Aldrich RP grade) were used as received. Ultrapure water (resistivity: 18.2 MΩ/cm at 25 °C) was obtained with Sarium® pro Ultrapure water purification Systems, Sartorius Stedim. Dialysis membrane, SpectraPor® 1, MWCO 6–8 kDa (Spectrum Laboratories, Inc., Piscataway, NJ, USA) was soaked in distilled water for 2 h and then thoroughly rinsed before use. LiF crystals, 15 × 15 mm^2 and 1 mm thick, polished on the larger opposite faces, were purchased by MaTecK - Material-Technologie & Kristalle GmbH.

2.2. Microgel synthesis

Two PNIPAM microgels with different size were synthesised via precipitation polymerisation by varying the SDS amount in the reaction feed [35]. For the synthesis of large particles, 3.716 g of NIPAM and 0.065 g of BIS were solubilised in 230 mL of ultrapure water and transferred into a 250 mL four-necked jacketed reactor equipped with condenser and mechanical stirrer. The solution was deoxygenated by purging with nitrogen for 1 h and heated at 70 °C. The addition of 0.161 g of KPS, dissolved in 10 mL of deoxygenated water, started the polymerisation, that was stopped after 4 h. For the synthesis of small particles, the same procedure and NIPAM/BIS molar ratio was used, but SDS (7.82 mM) was also added in the feed of the reaction to reduce the particles diameter. At the end of the synthesis, both microgel dispersion were purified by dialysis with a MWCO 6–8 kDa membrane against distilled water with frequent changes for two weeks. Through gravimetric measurements, the final weight concentration C_w of large and small PNIPAM microgel was determined to be ~1%. To prepare samples at higher concentrations, a cycle of lyophilisation to dryness and redispersion in H_2O was performed. Samples at different concentrations were obtained by dilution from the solution at C_w = 10%.

2.3. Preparation of thin films

Thin films of PNIPAM microgels were deposited on LiF crystals using a standard spin-coater (Polos SPIN150i/200i infinite). Before film deposition, the LiF crystals underwent thermal treatments at the temperatures T = 500 °C and 700 °C for 2 h in a muffle furnace to improve their surface quality. 50 μL of aqueous suspensions of PNIPAM microgel at three different weight concentrations (C_w = 1%, 3%, 5%) were deposited on LiF crystal substrates (at zero rotation) and spin-coated through a two-step deposition process. Two deposition protocols were adopted setting the first step spin speed (ω_1) at 500 rpm and 1500 rpm, while keeping constant the spin speed of the second step (ω_2) was kept constant at 5000 rpm (see Table 1). The spin speeds of the two steps where optimised to obtain thin and homogeneous films.

2.4. Proton irradiation

The LiF crystals coated with PNIPAM microgel films were irradiated perpendicularly with almost monochromatic, collimated proton beams produced by the vertical extraction line of the TOP-IMPLART linear accelerator under operation and development at ENEA Frascati [36]. The vertical beamline was designed for *in vitro* radiobiology studies to allow in air irradiation of cell monolayers placed perpendicularly to the beam direction. The crystals were irradiated with a single pulse of protons of energy E≈1 MeV and total average charge Q = 1 pC.

2.5. Characterisation

Dynamic light scattering. Dynamic Light Scattering (DLS) measurements were performed with an optical setup equipped with a solid-state laser with wavelength of 632.8 nm (power of 10 mW) and a single-mode collecting fibre at the scattering angle θ = 90°. The intensity auto-correlation functions $g_2(Q,t) = \frac{\langle I(Q,0)I(Q,t)\rangle}{\langle I(Q,0)\rangle^2}$ were therefore calculated at $Q = (4\pi n/\lambda)\sin(\theta/2)$ and fitted through the Kohlrausch-Williams-Watts expression [37,38] $g_2(Q,t) = 1 + b[e^{-(t/\tau(Q))^{\beta}}]^2$, where b is the coherence factor, τ is an "effective" relaxation time and β describes the deviation from the simple exponential decay (β = 1), usually found in monodisperse systems, giving a measure of the relaxation time distribution due to the intrinsic sample polydispersity. DLS measurements were performed in the temperature range T = (20–40) °C at low weight concentration (C_w = 0.01%) to obtain the hydrodynamic diameters. Indeed, in the high dilution limit, the particle hydrodynamic diameter D_H can be estimated from relaxation time τ of the intensity correlation functions $g_2(Q,t)$, using the Stokes-Einstein relationship:

$$D_H = \frac{k_B T}{3\pi\eta D_t} \quad (1)$$

where k_B is the Boltzman constant, T is the sample temperature, D_t is the translational diffusion coefficient from the relation $\tau = 1/Q^2 D_t$ and η is the sample viscosity that can be approximated to that of the solvent.

UV-vis-NIR spectroscopy. Hemispherical optical transmittances of microgel films on LiF crystals were measured using the UV-Vis-NIR spectrophotometer Perkin Elmer Lambda 1050+ equipped with an integrating sphere. Measurements were performed in the wavelength range λ = (220–2000) nm at 1 nm resolution and room temperature for thin films of PNIPAM microgels spin-coated at three weight concentrations (C_w = 1%, 3%, 5%) on LiF crystals. Data reproducibility was tested for each sample.

Atomic force microscopy. For the investigation of the morphological properties of both substrates and films, AFM measurements were performed using the A100 PLUS AFM (A.P.E. Research s.r.l., Area Science Park, Basovizza (TS), Italy) and a hybrid system made of a commercial head (SMENA, NT-MDT), home-built electronics and a digital lock-in amplifier (Zurich HF2LI), both operating in contact and non-contact mode. All images were taken in non-contact mode, in air ambient conditions, with commercial MikroMasch cantilevers HQ:NSC15 (nominal force constant from 20 to 80 N/m and resonance frequency from 265 to 410 kHz) and HQ:NSC35 (nominal force constant from 5.4 to 16 N/m and resonance frequency from 130 to 300 kHz). For topography and statistical analysis the open source software Gwyddion was used [39].

Contact-angle setup. For investigating the wetting properties of the substrates used for PNIPAM microgel deposition, a specific *in-house* optical setup for contact angle measurements was employed. The setup consists of a fibre illuminator that backlights the sample through a diffuser, an adjustable sample holder on which the substrate is placed, and a portable Dino-Lite AM4515ZT digital microscope [40] connected to a computer with the dedicated software DinoCapture 2.0. This setup allows for the visualisation of the magnified droplet image and facilitates the analysis for contact angle measurements.

Fluorescence microscopy. To visualise the fluorescent tracks induced by single protons in irradiated LiF crystals, a Nikon Eclipse 80-i fluorescence microscope was used, equipped with a mercury lamp, a Nikon TU Plan Fluor 100× objective (numerical aperture 0.9), and a −30 °C cooled s-CMOS Andor NEO camera for acquiring 16-bit grayscale images at 2560 × 2160 pixels. A Chroma ET440/40x excitation filter was used to select a ≈40 nm wide wavelength range within the broad absorption band of the CCs and an ET610lp emission filter was used to spectrally integrate the light emitted from the F_2 CCs only (at wavelengths above 610 nm), to optimise the signal-to-noise ratio in the images.

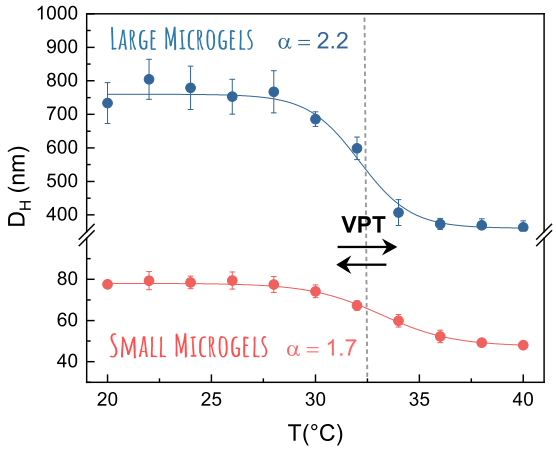

Fig. 1. Hydrodynamic diameters of small and large microgels obtained from DLS measurements as a function of temperature.

3. Results and discussion

Two different PNIPAM microgels were synthesised through radical precipitation polymerisation following the protocol reported in Ref. [6, 31]. Particles of different sizes were obtained by adding the surfactant SDS in one case and at zero SDS content in the second case. In both cases a relatively low crosslinker-to-monomer ratio (BIS/NIPAM) of 1.3 mol% was chosen to achieve soft and deformable particles, allowing for the formation of a densely packed film of nanoparticles with uniform and continuous coverage of the substrate.

Particle sizes of both microgel suspensions were investigated through DLS measurements in the high dilution limit (C_w = 0.01%), over a temperature range from 20 °C to 40 °C. The temperature behaviour of the hydrodynamic diameter of the microgel particles is shown in Fig. 1, where it is clear that microgels of two different sizes are obtained by changing the surfactant concentration during the synthesis process. In particular, microgels with D_H(20 °C) = (78 ± 1) nm are obtained by adding SDS during the synthesis, while larger microgels with D_H(20 °C) = (734 ± 61) nm are obtained in the absence of SDS. For both systems, the transition from the swollen to the shrunken state occurs at about 32 °C. For large microgels, the swelling ratio α, defined as the volume ratio between swollen and shrunken states ($\alpha = V_{swollen}/V_{shrunken} = (D_H(20\,°C)/D_H(40\,°C))^3$) [41], is greater than that for small microgels ($\alpha \approx 2.2$ and $\alpha \approx 1.7$, respectively), indicating a higher shrinking capability that can be related to a higher particle softness.

The optimised deposition protocols previously investigated by our group for microgel films spin-coated on standard substrates, such as glass [42], have been implemented for LiF crystal coatings. In this case, a non-trivial interaction between LiF crystals and PNIPAM microgels emerged, primarily due to the delicate balance between hydrophilic and hydrophobic nature of the substrate and to the local inhomogeneities characterising the crystal surface. Deposition tests on pristine LiF crystals resulted in highly heterogeneous films due to the presence of residuals and scratches on the crystal surface as a result of the polishing procedure. Improving the surface quality of the LiF substrates is imperative to obtain smooth and homogeneous microgel films. Moreover, for the application of the LiF crystals as FNTDs, the signal-to-noise ratio must be optimised to improve the detection of the photoluminescent signal emitted from CCs induced by ionising radiation. To this aim the crystals were thermally treated with an annealing process at a temperature of 500 °C and 700 °C for 2 h in a muffle furnace before microgel film deposition. The effect of thermal treatments on the wettability properties of LiF crystals were investigated by the *in-house* contact-angle setup. It is indeed well known that microgel adhesion and flattening on the substrate depend on the balance between adhesion energy, particle softness and deposition process. In particular, greater spreading and adhesion of microgels on a solid substrate is expected at increasing hydrophobicity, since it is driven by shielding of weak water-substrate interactions [33,43]. Tailoring the surface energy of the substrate to match the microgel properties can improve wetting and enhance the overall coating performances. To test the surface wettability, a water droplet of V=10 μL was deposited on the pristine and on the thermally treated LiF crystals surfaces. In Fig. 2 the results from the contact-angle measurements before (Fig. 2(a)) and after thermal treatments at T = 500 °C (Fig. 2(b)) and T = 700 °C (Fig. 2(c)) are reported. Values of contact angles between water droplet and LiF crystals of θ = (88 ± 1)°, θ = (76 ± 2)° and θ = (75 ± 3)° were respectively obtained. These results suggest a rather hydrophobic nature of LiF crystals with respect to conventional glass substrates that can be slightly changed through thermal treatments, representing a new control parameter for microgel film adhesion and stability.

The effects of thermal treatments on the LiF crystal surface were investigated through AFM measurements. AFM images acquired over a 10× 10 μm^2 area for pristine LiF crystals (Fig. 2(d)) and LiF crystals after thermal treatment at T = 500 °C and T = 700 °C (Fig. 2(e) and (f)) confirmed the possibility to efficiently remove residues from the materials used to polish the crystal faces and any scratches on the surface. However, treatments at 500 °C did not completely eliminate residual contaminants on the LiF crystal surface, while treatments at 700 °C yielded the best results. Moreover, thermal treatments were observed to slightly increase LiF crystal surface roughness. Root Mean Square (RMS) roughness values of RMS = (4.1 ± 0.2) nm were found for pristine LiF crystals, while roughness values of RMS = (5.2 ± 0.1) nm and RMS = (5.8 ± 0.2) nm were found for LiF crystal thermally treated at T = 500 °C and 700 °C, respectively.

It is well known that the solid substrate topography, including its roughness and porosity, can impact the microgel coating. Finding the best compromise between surface roughness and uniformity is therefore crucial. Indeed, rough surfaces may provide additional sites for microgel adhesion, improving coating stability, while excessively rough surfaces could lead to uneven coatings, affecting thin film optical and mechanical properties.

In order to investigate the effect of thermal treatments on the film topography, microgel suspensions were spin-coated on pristine and thermally treated LiF crystals at different concentrations and through different deposition protocols (Table 1). Fig. 3 reports an example of AFM images acquired over a 10 × 10 μm^2 area for large microgel films at C_w = 3% spin-coated through the deposition protocol n.1 on pristine LiF crystal and on LiF crystals after thermal treatment at T = 500 °C and T = 700 °C, as an example. Thermal treatments allow to obtain more homogeneous and smoother microgel films with RMS roughness values decreasing from RMS = (19 ± 5) nm to RMS = (11 ± 3) nm on pristine and pre-annealed LiF crystals at 700 °C, respectively. These changes are accompanied by a decrease of the microgel height probably due to surface defect removal upon thermal treatment. To investigate the role of weight concentration on microgel arrangement on the surface, thin films of both large and small microgel particles were obtained by spin-coating the same volume of aqueous suspensions of PNIPAM microgel at C_w = 1%, 3% and 5% on pre-annealed LiF crystals through both the double-step deposition protocols. For their application in photoluminescent solid-state radiation detectors, high-transparency in the visible spectral region is required, therefore the obtained thin films were characterised through UV-Vis-NIR spectrophotometry, in the range of wavelengths between 220 nm and 2000 nm. In Fig. 4 the hemispherical optical transmittance spectra at room temperature of the microgel films deposited at different weight concentrations on LiF crystals thermally treated at T = 500 °C, are reported as an example together with the transmittance spectra of the LiF crystal. UV-Vis-NIR spectrophotometric measurements confirmed the possibility to obtain transparent microgel films on LiF crystals in the whole wavelength range from the ultraviolet to the infrared region. The slightly lower

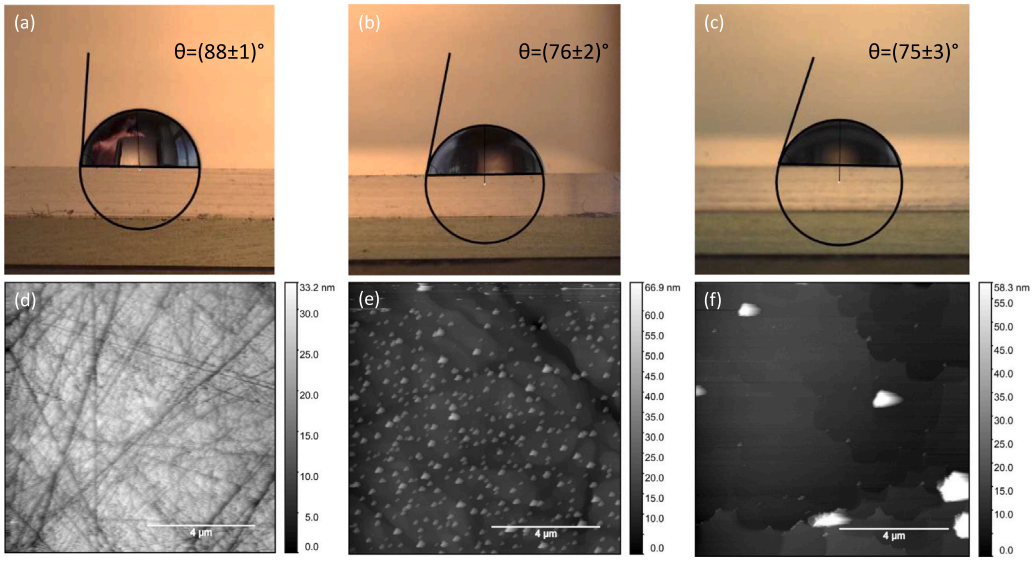

Fig. 2. Contact angle measurements on (a) pristine LiF crystals and LiF crystals after thermal treatment at (b) T = 500 °C and (c) T = 700 °C. AFM images acquired over a 10 × 10 μm^2 area for (d) pristine LiF crystals and LiF crystals after thermal treatment at (e) T = 500 °C and (f) T = 700 °C.

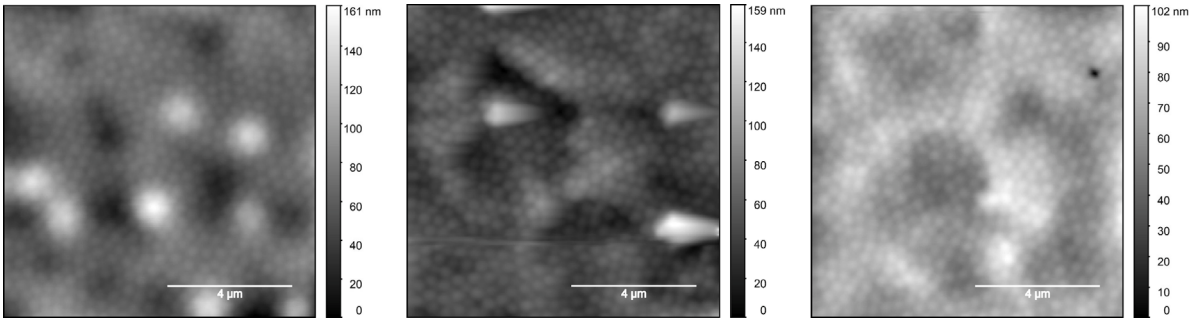

Fig. 3. AFM images acquired over a 10× 10 μm^2 area for large microgel films deposited through spin-coating on (a) pristine LiF crystals and LiF crystals after thermal treatment at (b) T = 500 °C and (c) T = 700 °C.

transmittance with respect to that of the LiF crystal suggests a refractive index of microgel films higher than that of the uncoated crystal, that is one of the most transparent materials in nature with a very low refractive index n ≈ 1.39 at 640 nm.

UV-Vis-NIR transmittance measurements suggested the possibility to obtain more uniform and transparent films by increasing weight concentration as a consequence of the more homogeneous packing of microgel particles on the substrate. This hypothesis has been corroborated by AFM measurements. In Fig. 5 AFM images acquired over a 10 × 10 μm^2 area for large microgels spin-coated on pre-annealed LiF crystals through a double step protocol with ω_1 = 500 rpm/s and ω_2 = 5000 rpm/s (deposition protocol n.2) at three different concentrations (C_w = 1%, 3% and 5%) are reported.

Statistical quantities obtained from their analysis are reported in Table 2 for films obtained through the spin-coating protocols n.1 and n.2 (Table 1). From these results we can speculate that the surface roughness decreases with weight concentrations, while grain number increases with increasing C_w. Moreover, the decrease of the mean grain size with C_w can be correlated to the lower interparticle distances and a more highly-packed structure of highly concentrated films that guarantees a higher coverage degree of the solid surface. The investigation of the concentration-dependent morphological properties allows to identify concentrations C_w = 3% and C_w = 5% as the most suitable ones for LiF crystal coatings. However, mechanical and morphological properties of microgel films are expected to depend on the particle size as a result of their intra-particle structure and of inter-particle interactions.

Table 2
Statistical quantities obtained from AFM images for thin films of PNIPAM microgels at C_w = 1%, 3% and 5% deposited through protocol n.1 and n.2.

Protocol number	C_w	RMS roughness (nm)	Grain number	Mean grain size (nm)
1	1%	20 ± 3	532	386 ± 4
1	3%	16 ± 4	684	352 ± 11
1	5%	3.3 ± 0.4	721	337 ± 7
2	1%	19 ± 7	564	318 ± 5
2	3%	14 ± 5	637	312 ± 7
2	5%	4 ± 1	666	284 ± 5

To explore the role of microgel size on film topography, aqueous suspensions of large and small microgels were spin-coated on LiF

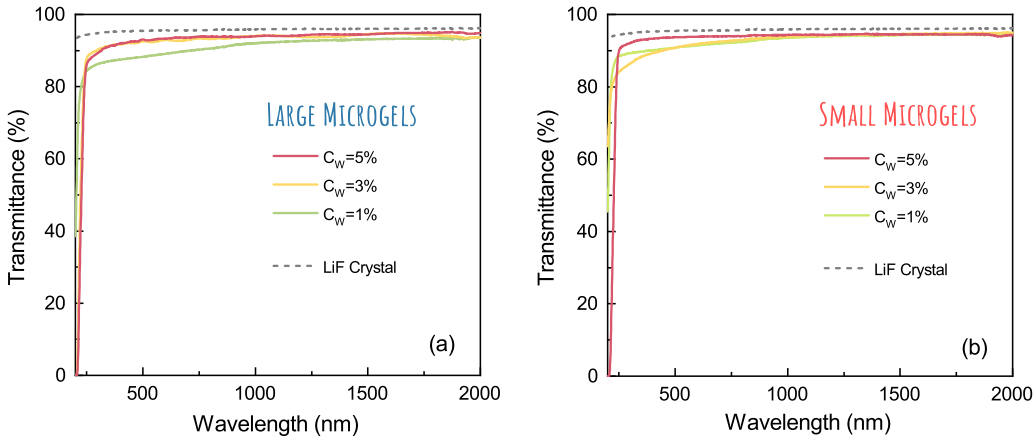

Fig. 4. Optical transmittance spectra of (a) large and (b) small PNIPAM microgel films of weight concentration C_w = 1%, 3%, 5% spin-coated on LiF crystals after thermal treatments at T = 500 °C, compared with the transmittance spectrum of the bare LiF crystal.

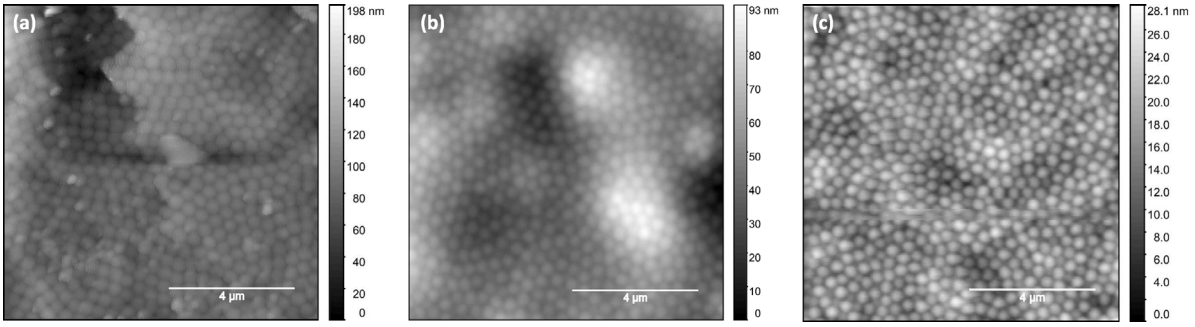

Fig. 5. AFM images acquired over a 10 × 10 µm^2 area for large microgel films spin-coated on LiF crystals after thermal treatment at T = 500 °C at (a) C_w = 1%, (b) C_w = 3% and (c) C_w = 5%.

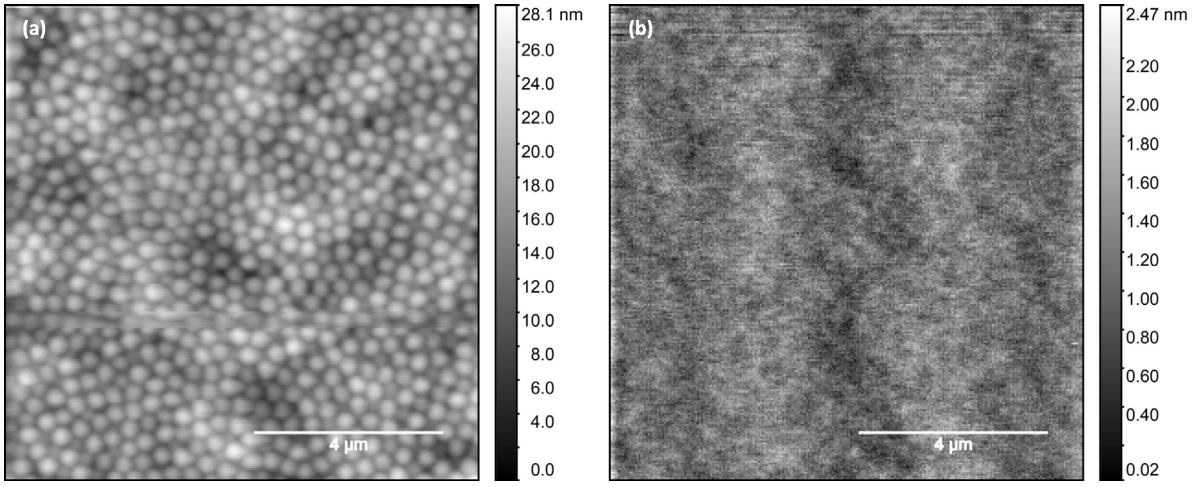

Fig. 6. AFM images acquired over a 10 × 10 µm^2 area for (a) large and (b) small microgel films at C_w = 5% spin-coated on LiF crystals pre-annealed at T = 500 °C.

crystals treated at T = 500 °C and 700 °C through the same deposition protocols. Fig. 6 shows a comparison between AFM images acquired over a 10 × 10 µm^2 area for large and small PNIPAM microgel films at concentration C_w = 5% deposited on a LiF crystal previously annealed at T = 500 °C, as an example. Large PNIPAM microgels (Fig. 6(a)) form films with a homogeneous and regular structure on the LiF crystals, arranging into a compact close-packed structure equivalent to that observed on glass substrate [42]. In this case large microgel particles have heights of the order of tens of nanometers indicating a high compression of the microgel on the solid surface and thus demonstrating their extreme softness and deformability at this low cross-linker concentration. Their softness offers the possibility to obtain very thin films up to a few tens of nanometers in monolayer configurations, an imperative requirement for their application as coating layer of photoluminescent solid-state detectors. A completely different behaviour is observed in small PNIPAM microgel films (Fig. 6(b)), as microgels with diameters of the order of a few tens of nanometers tend to interpenetrate, forming films where individual particles lose their spherical shape and are no longer distinguishable. At the same time their interpenetration yields

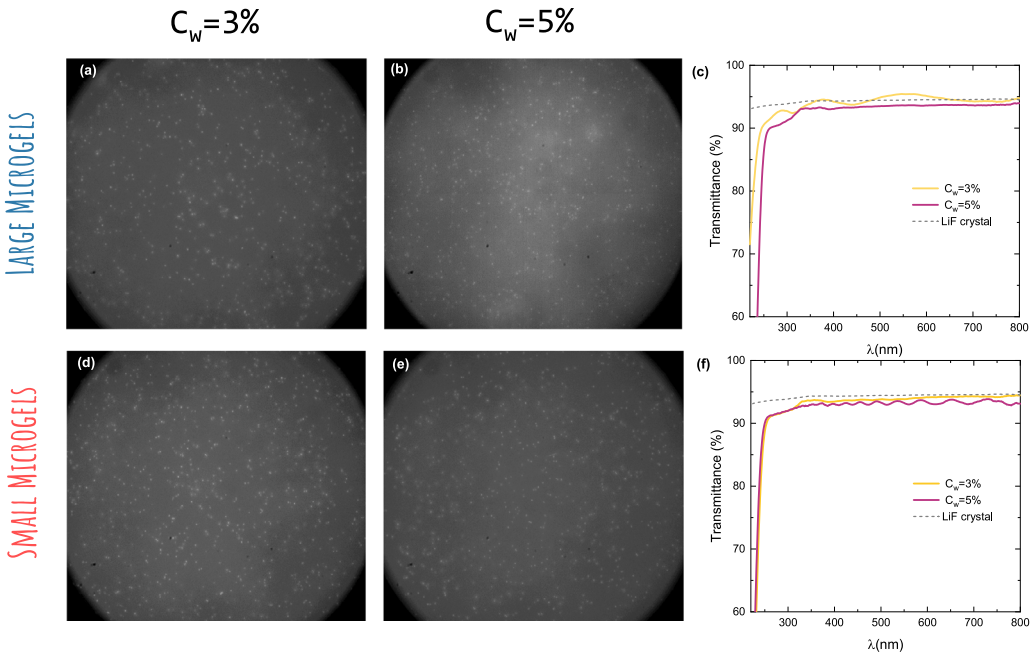

Fig. 7. Fluorescent images over a 167 × 167 μm^2 area of proton traces with a nominal energy of 3 MeV (single pulse with Q = 1 pC/pulse) in LiF crystals thermally treated at T = 700 °C and coated with large microgel films of (a) C_w = 3% and (b) C_w = 5%, and small microgel films of (c) C_w = 3% and (d) C_w = 5%.

to flat and continuous films with a high coverage degree of the solid substrate.

This systematic investigation of the optical and morphological properties of microgel films spin-coated on LiF crystals has allowed to define the ideal protocols for their integration on the LiF-based detectors. The double-step protocol with ω_1 = 1500 rpm and ω_2 = 5000 rpm was selected to deposit large and small microgel films at the two ideal concentrations (C_w = 3% and C_w = 5%) on LiF crystals previously subjected to thermal treatment for 2 h at 700 °C, aiming to remove deep scratches and reduce the background photoluminescence signal.

The obtained samples were irradiated under the same conditions with a single pulse of proton beam ≈1 MeV energy and a charge of Q = 1 pC/pulse and fluence Φ = 4.1 ± 0.1)×10^6 protons/cm^2. Fig. 7 shows images of the nuclear fluorescent tracks stored in LiF crystals coated with PNIPAM microgels and recorded at the fluorescence optical microscope equipped with a dedicated emission filter collecting the red luminescence at wavelengths above 610 nm, corresponding to the emission of the F_2 CCs. Using this filter, the fluorescent background is minimised since it is mainly due to a fluorescence signal in the green range of the visible spectrum, yielding to an increase of the signal-to-noise ratio and allowing to visualise the fluorescent nuclear tracks stored in all the LiF crystals coated with large (Fig. 7(a, b)) and small (Fig. 7(d, e)) PNIPAM microgel films at C_w = 3% and C_w = 5%. These results can be qualitatively correlated to the high hemispherical optical transmittances of the microgel films in the visible spectral range (Fig. 7(c) and (f)). Interestingly, the UV–Vis transmittance spectra of films of large microgels at C_w = 3% and small microgels at C_w = 5% showed the presence of interference fringes. This behaviour confirms the high uniformity of the microgel coatings on a large area and a good quality of the interface between microgel film and crystal surface that is improved by thermal treatments at 700 °C. Moreover, from the shape of the optical transmittances we can suppose a film thickness of hundreds of nanometers that can be controlled by concentration and microgel size and a not negligible difference between refractive indexes of the film and the substrate.

These results suggest that crystals subjected to thermal treatments at 700 °C offer a residual-free surface on which thin and uniform PNIPAM microgel films can be grown without significantly attenuating the photoluminescence intensity emitted by colour centres formed in LiF. However, the balance between microgel size, weight concentration and film thickness are additional control parameters for reducing background fluorescence affecting the signal-to-noise ratio.

4. Conclusions

PNIPAM microgels of two different sizes were obtained by adding different amounts of sodium dodecyl sulfate (SDS) during the synthesis procedure, as confirmed by DLS measurements. Microgel thin films were therefore obtained by spin-coating both large and small microgel suspensions at different weight concentrations on pristine and thermally-treated lithium fluoride crystals to explore the impact of the substrate on the optical and morphological properties of microgel films. Thermal treatments at temperature of 700 °C allowed to obtain high quality surfaces by efficiently removing any residues and scratches on the crystal surface that could affect the microgel coatings. To explore the impact of surface quality, microgel size and particle concentration on the microgel film properties, a systematic investigation was performed by combining wettability measurements, UV-Vis-NIR spectroscopy and Atomic Force Microscopy. By following a double-step spin-coating deposition protocol, uniform and smooth thin films with high transparency in the whole wavelength range from the visible to the near-infrared region were obtained. In particular, the hemispherical optical transmittance spectra confirmed the formation of thin and uniform films with low refractive index on such non-conventional substrates, thus unlocking new possibilities for microgel-coated materials. The obtained results demonstrate the possibility of exploiting PNIPAM microgel films to develop hybrid and potentially biocompatible detectors able to combine the high spatial resolution of LiF-based fluorescent nuclear track detectors with the PNIPAM versatility. Moreover, the first FNTDs irradiation tests confirmed the feasibility of using the obtained fluorescent nuclear track detectors for irradiations with proton energies of the order of few MeV and a fluence of the order of 10^6 protons/cm^2, ideal conditions for radiobiology experiments with low-energy proton beams on cell cultures.

CRediT authorship contribution statement

Valentina Nigro: Writing – review & editing, Writing – original draft, Visualization, Validation, Supervision, Resources, Methodology,

Investigation, Formal analysis, Data curation, Conceptualization. **Claudia Colantonio:** Investigation, Formal analysis, Data curation. **Massimo Piccinini:** Writing – review & editing, Validation, Methodology, Investigation, Formal analysis, Data curation. **Elena Buratti:** Writing – review & editing, Validation, Methodology, Investigation, Formal analysis, Data curation. **Riccardo Ciciotti:** Investigation, Formal analysis, Data curation. **Evaristo Cisbani:** Writing – review & editing. **Cinzia De Angelis:** Writing – review & editing. **Franco Dinelli:** Writing – review & editing, Investigation, Data curation. **Giuseppe Esposito:** Writing – review & editing. **Francesca Limosani:** Writing – review & editing, Investigation. **Enrico Nichelatti:** Writing – review & editing. **Concetta Ronsivalle:** Writing – review & editing. **Maria Aurora Vincenti:** Writing – review & editing. **Barbara Ruzicka:** Writing – review & editing, Validation, Supervision, Resources, Project administration, Conceptualization. **Rosa Maria Montereali:** Writing – review & editing, Validation, Supervision, Resources, Project administration, Funding acquisition, Conceptualization.

Declaration of competing interest

The authors declare that they have no known competing financial interests or personal relationships that could have appeared to influence the work reported in this paper.

Data availability

No data was used for the research described in the article.

Acknowledgements

We acknowledge financial support from Regione Lazio, L.R. 13/2008, BIOTRACK Project (Fluorescent Nuclear Track Detectors for Radiobiology) N.Prot. A0375-2020-36509.

References

[1] V. Nigro, R. Angelini, B. Rosi, M. Bertoldo, E. Buratti, S. Casciardi, S. Sennato, B. Ruzicka, Study of network composition in interpenetrating polymer networks of poly(n isopropylacrylamide) microgels: The role of poly(acrylic acid), J. Colloid Interface Sci. 545 (2019) 210–219, http://dx.doi.org/10.1016/j.jcis.2019.03.004.

[2] S. Franco, E. Buratti, B. Ruzicka, V. Nigro, N. Zoratto, P. Matricardi, E. Zaccarelli, R. Angelini, Volume fraction determination of microgel composed of interpenetrating polymer networks of pnipam and polyacrylic acid, J. Phys.: Condens. Matter. 33 (17) (2021) 174004, http://dx.doi.org/10.1088/1361-648X/abe1ec.

[3] R. Rivas-Barbosa, J. Ruiz-Franco, M.A. Lara-Peña, J. Cardellini, A. Licea-Claverie, F. Camerin, E. Zaccarelli, M. Laurati, Link between morphology, structure, and interactions of composite microgels, Macromolecules 55 (5) (2022) 1834–1843, http://dx.doi.org/10.1021/acs.macromol.1c02171.

[4] A.S. Caldwell, B.A. Aguado, K.S. Anseth, Designing Microgels for Cell Culture and Controlled Assembly of Tissue Microenvironments, Adv. Funct. Mater. 30 (37) (2020) 1907670, http://dx.doi.org/10.1002/adfm.201907670, arXiv:https://onlinelibrary.wiley.com/doi/pdf/10.1002/adfm.201907670.

[5] S. Schmidt, H. Motschmann, T. Hellweg, R. von Klitzing, Thermoresponsive surfaces by spin-coating of PNIPAM-co-PAA microgels: A combined AFM and ellipsometry study, Polymer 49 (3) (2008) 749–756, http://dx.doi.org/10.1016/j.polymer.2007.12.025.

[6] V. Nigro, R. Angelini, M. Bertoldo, E. Buratti, S. Franco, B. Ruzicka, Chemical-physical behaviour of microgels made of interpenetrating polymer networks of pnipam and poly(acrylic acid), Polymers 13 (9) (2021) http://dx.doi.org/10.3390/polym13091353.

[7] S. Wellert, M. Richter, T. Hellweg, R. von Klitzing, Y. Hertle, Responsive microgels at surfaces and interfaces, Z. Phys. Chem. 229 (7–8) (2015) 1225–1250, http://dx.doi.org/10.1515/zpch-2014-0568.

[8] L. Zhu, Y. Meng, J. Zhou, Y. Hu, S. Gao, S. Li, J. Liu, S. Wang, Y. Xia, Tough and transparent photonic hydrogel nanocomposites for display, sensing, and actuation applications, ACS Appl. Nano Mater. 6 (8) (2023) 6984–6991, http://dx.doi.org/10.1021/acsanm.3c00889.

[9] T. Shu, L. Hu, H. Hunter, N. Balasuriya, C. Fang, Q. Zhang, M.J. Serpe, Multi-responsive micro/nanogels for optical sensing, Adv. Phys. X 7 (1) (2022) 2043185, http://dx.doi.org/10.1080/23746149.2022.2043185.

[10] J. Kim, S. Nayak, L.A. Lyon, Bioresponsive hydrogel microlenses, J. Am. Chem. Soc. 127 (26) (2005) 9588–9592, http://dx.doi.org/10.1021/ja0519076.

[11] K. Marcisz, M. Karbarz, Z. Stojek, Electrochemical chemo- and biosensors based on microgels immobilized on electrode surface, Electrochem. Sci. Adv. 2 (5) (2022) e2100162, http://dx.doi.org/10.1002/elsa.202100162.

[12] S. Zahid, A.K. Alzahrani, N. Kizilbash, J. Ambreen, M. Ajmal, Z.H. Farooqi, M. Siddiq, Preparation of stimuli responsive microgel with silver nanoparticles for biosensing and catalytic reduction of water pollutants, RSC Adv. 12 (2022) 33215–33228, http://dx.doi.org/10.1039/D2RA05475B.

[13] Y. Xia, Y. Tang, X. He, F. Pan, Z. Li, H. Xu, J.R. Lu, Patterned thermoresponsive microgel surfaces to control cell detachment, Biomacromolecules 17 (2) (2016) 572–579, http://dx.doi.org/10.1021/acs.biomac.5b01507.

[14] I. Sanzari, E. Buratti, R. Huang, C.G. Tusan, F. Dinelli, N.D. Evans, T. Prodromakis, M. Bertoldo, Poly(n-isopropylacrylamide) based thin microgel films for use in cell culture applications, Sci. Rep. 10 (1) (2020) 6126, http://dx.doi.org/10.1038/s41598-020-63228-9.

[15] M. Flechner, J. Schaller, M. Stahl, K. Achberger, S. Gerike, Y. Hannappel, J. Fu, M. Jaeger, T. Hellweg, C. Duschl, K. Uhlig, Adhesion, proliferation, and detachment of various cell types on thermoresponsive microgel coatings, Biotechnol. Bioeng. 119 (7) (2022) 1728–1739, http://dx.doi.org/10.1002/bit.28095.

[16] L.V. Sigolaeva, D.V. Pergushov, M. Oelmann, S. Schwarz, M. Brugnoni, I.N. Kurochkin, F.A. Plamper, A. Fery, W. Richtering, Surface functionalization by stimuli-sensitive microgels for effective enzyme uptake and rational design of biosensor setups, Polymers 10 (7) (2018) 00, http://dx.doi.org/10.3390/polym10070791.

[17] A. Burmistrova, R. von Klitzing, Control of number density and swelling/shrinking behavior of p(nipam–aac) particles at solid surfaces, J. Mater. Chem. 20 (2010) 3502–3507, http://dx.doi.org/10.1039/B923969C.

[18] P. Bilski, B. Marczewska, W. Gieszczyk, M. Kłosowski, M. Naruszewicz, M. Sankowska, S. Kodaira, Fluorescent imaging of heavy charged particle tracks with LiF single crystals, J. Lumin. 213 (2019) 82–87, http://dx.doi.org/10.1016/j.jlumin.2019.05.007.

[19] P. Bilski, B. Marczewska, W. Gieszczyk, M. Kłosowski, T. Nowak, M. Naruszewicz, Lithium fluoride crystals as fluorescent nuclear track detectors, Radiat. Prot. Dosim. 178 (3) (2017) 337–340, http://dx.doi.org/10.1093/rpd/ncx116.

[20] M. Piccinini, E. Nichelatti, G. Esposito, E. Cisbani, F. Santavenere, P. Anello, V. Nigro, M. Vincenti, F. Limosani, C. Ronsivalle, A. Ampollini, C.D. Angelis, R. Montereali, Detection of fluorescent low-energy proton tracks in lithium fluoride crystals, Radiat. Meas. (2024) submitted.

[21] J. Schulman, W. Compton, Color Centers in Solids, Pergamon Press, Oxford, UK, 1963.

[22] S.W.S. McKeever, A Course in Luminescence Measurements and Analyses for Radiation Dosimetry, Wiley, 2022.

[23] K. Kawamura, M. Hirano, T. Kurobori, D. Takamizu, T. Kamiya, H. Hosono, Femtosecond-laser-encoded distributed-feedback color center laser in lithium fluoride single crystals, Appl. Phys. Lett. 84 (3) (2004) 311–313, http://dx.doi.org/10.1063/1.1640784.

[24] R.M. Montereali, M. Piccinini, E. Burattini, Amplified spontaneous emission in active channel waveguides produced by electron-beam lithography in LiF crystals, Appl. Phys. Lett. 78 (26) (2001) 4082–4084, http://dx.doi.org/10.1063/1.1381568.

[25] F. Bonfigli, A. Faenov, F. Flora, M. Francucci, P. Gaudio, A. Lai, S. Martellucci, R.M. Montereali, T. Pikuz, L. Reale, M. Richetta, M.A. Vincenti, G. Baldacchini, High-resolution water window X-ray imaging of in vivo cells and their products using LiF crystal detectors, Microsc. Res. Techn. 71 (1) (2008) 35–41, http://dx.doi.org/10.1002/jemt.20523.

[26] M. Piccinini, E. Nichelatti, C. Ronsivalle, A. Ampollini, G. Bazzano, F. Bonfigli, P. Nenzi, V. Surrenti, E. Trinca, M. Vadrucci, M. Vincenti, L. Picardi, R. Montereali, Visible photoluminescence of color centers in LiF crystals for advanced diagnostics of 18 and 27 MeV proton beams, Radiat. Meas. 124 (2019) 59–62, http://dx.doi.org/10.1016/j.radmeas.2019.03.010.

[27] E. Nichelatti, M. Piccinini, A. Ampollini, L. Picardi, C. Ronsivalle, F. Bonfigli, M.A. Vincenti, R.M. Montereali, Bragg-curve imaging of 7 MeV protons in a lithium fluoride crystal by fluorescence microscopy of colour centres, Europhys. Lett. 120 (5) (2018) 56003, http://dx.doi.org/10.1209/0295-5075/120/56003.

[28] M. Piccinini, E. Nichelatti, A. Ampollini, G. Bazzano, C. De Angelis, S. Della Monaca, P. Nenzi, L. Picardi, C. Ronsivalle, V. Surrenti, E. Trinca, M. Vadrucci, M. Vincenti, R. Montereali, Dose response and bragg curve reconstruction by radiophotoluminescence of color centers in lithium fluoride crystals irradiated with 35 MeV proton beams from 0.5 to 50 gy, Radiat. Meas. 133 (2020) 106275, http://dx.doi.org/10.1016/j.radmeas.2020.106275.

[29] M. Niklas, A. Abdollahi, M.S. Akselrod, J. Debus, O. Jäkel, S. Greilich, Subcellular spatial correlation of particle traversal and biological response in clinical ion beams, Int. J. Radiat. Oncol. Biol. Phys. 87 (5) (2013) 1141–1147, http://dx.doi.org/10.1016/j.ijrobp.2013.08.043.

[30] S. Kodaira, T. Konishi, A. Kobayashi, T. Maeda, T.A.F.T. Ahmad, G. Yang, M.S. Akselrod, Y. Furusawa, Y. Uchihori, Co-visualization of DNA damage and ion traversals in live mammalian cells using a fluorescent nuclear track detector, J. Radiat. Res. 56 (2) (2014) 360–365, http://dx.doi.org/10.1093/jrr/rru091.

[31] E. Buratti, I. Sanzari, F. Dinelli, T. Prodromakis, M. Bertoldo, Formation and stability of smooth thin films with soft microgels made of poly(n-isopropylacrylamide) and poly(acrylic acid), Polymers 12 (11) (2020) http://dx.doi.org/10.3390/polym12112638.

[32] S. Schmidt, M. Zeiser, T. Hellweg, C. Duschl, A. Fery, H. Möhwald, Adhesion and mechanical properties of pnipam microgel films and their potential use as switchable cell culture substrates, Adv. Funct. Mater. 20 (19) (2010) 3235–3243, http://dx.doi.org/10.1002/adfm.201000730.

[33] L. Hoppe Alvarez, A.A. Rudov, R.A. Gumerov, P. Lenssen, U. Simon, I.I. Potemkin, D. Wöll, Controlling microgel deformation via deposition method and surface functionalization of solid supports, Phys. Chem. Chem. Phys. 23 (2021) 4927–4934, http://dx.doi.org/10.1039/D0CP06355J.

[34] V. Nigro, R. Angelini, E. Buratti, C. Colantonio, R. D'Amato, F. Dinelli, S. Franco, F. Limosani, R.M. Montereali, E. Nichelatti, M. Piccinini, M.A. Vincenti, B. Ruzicka, Influence of a solid surface on pnipam microgel films, Gels 10 (7) (2024) http://dx.doi.org/10.3390/gels10070473, URL https://www.mdpi.com/2310-2861/10/7/473.

[35] W. McPhee, K.C. Tam, R. Pelton, Poly(n-isopropylacrylamide) latices prepared with sodium dodecyl sulfate, J. Colloid Interface Sci. 156 (1) (1993) 24–30, http://dx.doi.org/10.1006/jcis.1993.1075.

[36] L. Picardi, A. Ampollini, G. Bazzano, E. Cisbani, F. Ghio, R.M. Montereali, P. Nenzi, M. Piccinini, C. Ronsivalle, F. Santavenere, V. Surrenti, E. Trinca, M. Vadrucci, E.W. Tafo, Beam commissioning of the 35 MeV section in an intensity modulated proton linear accelerator for proton therapy, Phys. Rev. Accel. Beams 23 (2020) 020102, http://dx.doi.org/10.1103/PhysRevAccelBeams.23.020102.

[37] R. Kohlrausch, Theorie des elektrischen rckstandes in der leidener flasche, Ann. Phys., Lpz. 2 (1854) 179–214.

[38] G. Williams, D.C. Watts, Non-symmetrical dielectric relaxation behavior arising from a simple empirical decay function, J. Chem. Soc. Faraday Trans. 66 (1970) 80–85.

[39] Gwyddion. URL www.gwyddion.net.

[40] Dino-lite digital microscope, https://www.dino-lite.eu/en/.

[41] V. Nigro, B. Ruzicka, B. Ruta, F. Zontone, M. Bertoldo, E. Buratti, R. Angelini, Relaxation. dynamics, softness, And fragility of microgels with interpenetrated polymer networks, Macromolecules 53 (2020) 1596–1603.

[42] V. Nigro, E. Buratti, F. Limosani, R. Angelini, F. Dinelli, S. Franco, E. Nichelatti, M. Piccinini, M.A. Vincenti, R.M. Montereali, B. Ruzicka, Spin-coating deposition of thermoresponsive microgel thin films, Colloids Surf. A 674 (2023) 131918, http://dx.doi.org/10.1016/j.colsurfa.2023.131918.

[43] L. Hoppe Alvarez, S. Eisold, R.A. Gumerov, M. Strauch, A.A. Rudov, P. Lenssen, D. Merhof, I.I. Potemkin, U. Simon, D. Wöll, Deformation of microgels at solid–liquid interfaces visualized in three-dimension, Nano Lett. 19 (12) (2019) 8862–8867, http://dx.doi.org/10.1021/acs.nanolett.9b03688.